CrossMark

Organomontmorillonite-modified soybean oil-based polyurethane/epoxy resin interpenetrating polymer networks (IPNs)

Ke Xu[1] · Ru Chen[1] · Chengshuang Wang[2] · Yifan Sun[1] · Jing Zhang[1] ·
Ya Liu[1] · Hongfeng Xie[1] · Rongshi Cheng[1,3]

Abstract In this work, in order to investigate the reinforcement effects of organomontmorillonite (OMMT) in soybean oil-based polyurethane (PU)/epoxy (EP) interpenetrating polymer networks (IPNs), a series of OMMT-modified PU/EP IPNs were prepared. The impacts of OMMT on the structure, morphology, glass transition, damping properties, thermal stability, and mechanical properties of the PU/EP IPNs were characterized by X-ray diffraction, scanning electronic microscope, dynamic mechanical analysis, thermogravimetry analysis, and tensile test. Results reveal that the addition of OMMT increases the glass transition temperature of the PU/EP IPNs. However, the damping properties of the PU/EP IPNs are lowered with the incorporation of OMMT. The addition of OMMT heightens the thermal stability of the PU/EP IPNs. Tensile tests show that the addition of OMMT significantly increases the tensile strength and tensile modulus of the PU/EP IPNs. With 4 and 6 % loading of OMMT, the tensile strength and tensile modulus increase 64 and 391 %, respectively.

✉ Hongfeng Xie
hfxie@nju.edu.cn

1 MOE Key Laboratory of High Performance Polymer Materials and Technology (Nanjing University), School of Chemistry and Chemical Engineering, Nanjing University, Nanjing 210093, China

2 Department of Polymer Materials and Engineering, School of Materials Engineering, Yancheng Institute of Technology, Yancheng 224051, China

3 College of Material Science and Engineering, South China University of Technology, Guangzhou 510641, China

Introduction

Epoxy (EP) resins are one of the most versatile thermosetting polymers with diverse applications such as coatings, adhesives and composite materials due to their high mechanical strength and modulus, good thermal, adhesive, and electrical properties, outstanding moisture, chemical, and corrosion resistance, no volatiles emission and dimensional stability [1–3]. Except for these favorable properties, the major disadvantages are their poor impact and peel properties attributed to their brittle nature at room temperature. Hence, toughening agents are chosen to improve the toughness of epoxy materials for many end-use applications. The tougheners for epoxy include liquid rubbers, core–shell particles, and thermoplastics [4–6].

Recently, much attention has been paid to improving the toughness of epoxy resin with interpenetrating polymer networks (IPNs). The IPN is a combination of at least two polymers in network form, and at least one polymer is cross-linked at the presence with the other one with synergistic effect of advantages of each polymer. [7–10]. Because of its flexible and versatile structure, polyurethane (PU) has become one of the most commonly used polymers to generate IPNs with epoxy resin [11, 12]. More recently, increasing interests have been attracted to vegetable oil-based polyurethanes, because feedstocks are cheap and available in large quantities [13–17]. Vegetable oil-based polyurethanes have the advantages of low curing temperature, anti-corrosion, electrical insulation, and shape memory, while they are also biodegradable and biocompatible

🙋 Springer

[18]. Some attempts have been made to develop vegetable oil-based PU/EP IPNs [19–21].

Montmorillonite (MMT), whose general chemical formula is $M_x(Al_{4-x}Mg_x)Si_8O_{20}(OH)_4$, belongs to the structural family of 2:1 phyllosilicates [22]. Its crystal lattice consists of two-dimensional layers where a central octahedral sheet of alumina or magnesia is fused to two external silica tetrahedrons by the tip [22, 23]. Between the layer gaps of montmorillonite, there are exchangeable cations. If these hydrated cations are exchanged with organic cationic surfactants, the organomontmorillonite (OMMT) will become organophilic and more convenient for polymer modification. For decades, montmorillonite interests researchers due to the significant effects in polymer reinforcement [24] as well as its low cost. Polymer–montmorillonite nanocomposite systems have been researched with PU/EP IPNs [25–27]. Jia et al. found that OMMT improved the tribological performance and water resistance of the PU/EP IPNs. The glass transition temperature (T_g) of the PU/EP IPNs increased with the OMMT loading up to 3 mass% and then decreased with further increase in OMMT loading [28, 29]. Bakar et al. studied the effect of MMT on the properties of PU/EP IPNs with different polyols. The addition of 2 mass% MMT led to a tenfold increase in the flexural strain at break [30]. Li reported that the T_g and thermal stability of castor oil-based polyurethane/EP IPNs increased with the increase in OMMT loading. In addition, PU/EP IPNs and OMMT exhibited synergistic effect on improvement of tensile strength and toughness of pure EP [31]. Chen et al. investigated the effect of MMT on the damping, thermal, and mechanical properties of castor oil-based PU/EP IPNs. They observed that the incorporation of MMT enhanced the damping properties and thermal stability of castor oil-based PU/EP IPNs. Furthermore, the addition of MMT significantly improved the tensile strength and impact strength of IPNs [26]. To our knowledge, however, few works have been carried out on the effect of MMT on the properties of soybean oil-based PU/EP IPNs.

In our previous work [32], a series of soybean oil-based PU/EP IPNs were prepared. Moreover, the thermal, mechanical, and morphological properties of IPNs were studied. The optimized mass ratio between soybean oil-based PU and EP was obtained. In present paper, OMMT was incorporated in the soybean oil-based PU/EP IPN. The effects of OMMT on the physical properties of soybean oil-based PU/EP IPN were investigated.

Experimental

Materials

Epoxidized soybean oil (ESO) containing 5.3 % oxygen was provided by the Xiamen Vive Material Co., Ltd.

(Xiamen, China). Isophorone diisocyanate (IPDI) was provided by Creanova Spezialchemie, Germany. Methanol, ammonia (30 %), tetrafluoroboric acid (48 %), petroleum ether, and acetone were purchased from Nanjing Chemical Reagent Co., Ltd., China. Diglycidyl ether of bisphenol A (DGEBA)-based epoxy resin with an epoxide equivalent mass of 183–194 g mol^{-1} was purchased from Nantong Xingchen Synthetic Material Co., Ltd., China. Polyether amine (Jeffamine T403) was used as a curing agent, which purchased from Huntsman Corporation, USA. The chemical structure of ESO, IPDI, Jeffamine T403, and DGEBA is demonstrated in Fig. 1. The OMMT was supplied by Zhejiang Fenghong New Material Co., Ltd. (China). The OMMT is Na^+-montmorillonite ion changed with dioctadecyl dimethyl ammonium bromide, in which cation exchange capacity (CEC) is 100 $\sim$ 120 meq 100 g^{-1}. The physical characteristic of OMMT is shown in Table 1.

Preparation of soybean oil-based polyols

Soybean oil-based polyols were synthesized according to Ref. [33], giving polyols with a hydroxyl number of 137 mg KOH g^{-1}. The prepared polyols were shortened as polyol-137.

Synthesis of OMMT-modified PU/EP IPNs

OMMT-modified PU/EP IPNs were synthesized according to Ref. [17]. Polyol-137 was mixed with IPDI with the ratio $n_{(-NCO)}:n_{(-OH)} = 1:2$. The mixture was kept stirring at 90 °C for 1 h in N_2 atmosphere to form the soybean oil-based PU prepolymer. After cooling to room temperature, it was then mixed with DGEBA with a mass ratio of 30:70. The suspension of OMMT in dry acetone which had been sonicated at 100 W for 1 h was added into the PU/EP mixture, stirred, and then sonicated for 1 h. Acetone was then removed at 90 °C. T403 was added and sonicated for another 30 min. The mixtures were poured into polytetrafluoroethylene molds and were thermally treated at 90 °C for 2 h and 110 °C for 3 h to complete the reaction. The samples were naturally cooled down and remolded. The mass ratios of OMMT in this research were 0, 1, 2, 4, and 6 %, respectively, and denoted as OMMT-0, OMMT-1, OMMT-2, OMMT-4, and OMMT-6.

Characterization

Tensile test

Tensile properties were examined using a universal testing machine (Instron 4466) with a strain rate of 50 mm min^{-1} at 23 °C according to ASTM D638. The results were averaged over at least four specimens.

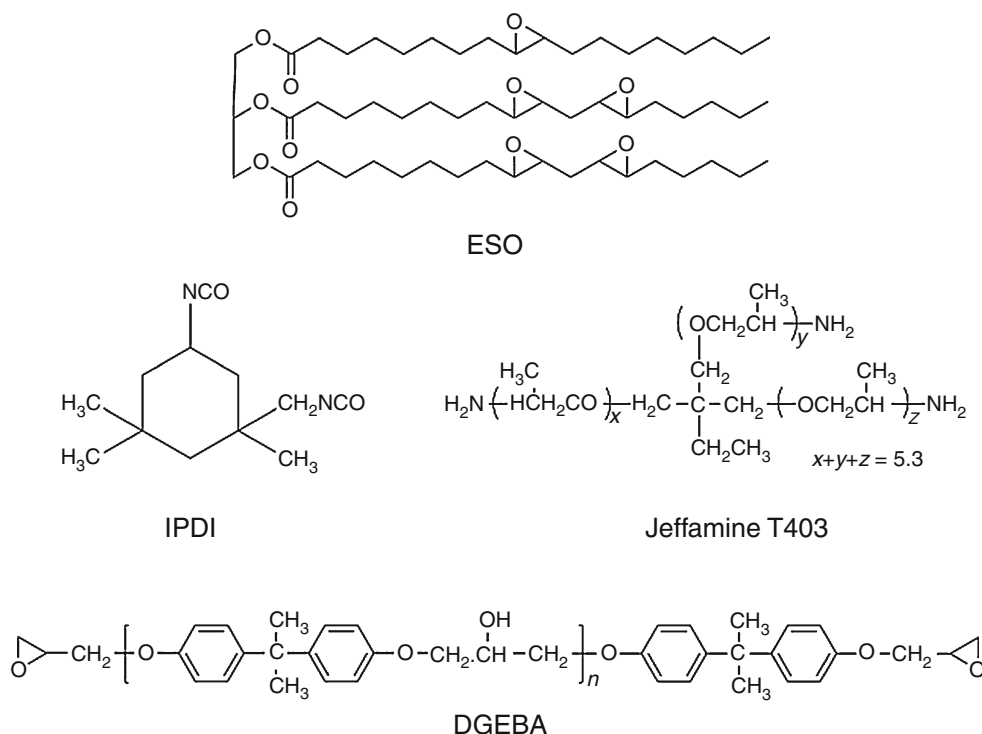**Fig. 1** Chemical structures of ESO, IPDI, Jeffamine T403, and DGEBA

ESO

IPDI

Jeffamine T403

$x+y+z = 5.3$

DGEBA

Table 1 Properties of OMMTs

Color	Particle size of dry powder/mesh	Laminated thickness/nm	Apparent density/g cm^{-3}	Humidity ratio/%	OMMT content/%	Diameter–thickness ratio
White	200	<25 nm	0.25–0.35	<3	96–98 %	200

Thermogravimetric analysis

Thermogravimetric (TG) analysis was measured using a Perkin-Elmer Pyris 1 TGA analyzer with a heating rate of 20 °C min^{-1} under a nitrogen atmosphere of 25–550 °C.

Dynamic mechanical analysis

The glass transition temperatures were studied by dynamic mechanical analysis (DMA; DMA + 450, 01 dB-Metravib). The measurements were performed from −50 to 100 °C under a tension mode with a heating rate of 3 °C min^{-1} and a frequency of 5 Hz.

X-ray diffraction

X-ray diffraction (XRD) study was carried out on a Shimadzu XRD-6000 using crystal monochromated Cu Kα radiation over the range $5° < 2\theta < 60°$ at a scanning rate of 6° min^{-1}.

Scanning electron microscopy

The morphology of the samples was observed by a scanning electron microscopy (SEM) instrument (S-4800, Hitachi). The samples were fractured in liquid nitrogen, and then the fractured surface of the samples was coated with gold before SEM observation.

Results and discussion

X-ray diffraction

X-ray diffraction is an effective method to probe the distances between clay layers. The XRD curves of OMMT and OMMT-modified soybean oil-based PU/EP IPNs are shown in Fig. 2, in which a comparison of diffraction angles between the clay and the modified IPNs is made. According to Bragg's law ($n\lambda = 2d \sin\theta$), diffraction angles are transferred into the layer distances of OMMT. As shown in Fig. 2, the d_{001} reflection peak of OMMT appears at 4.92° (2θ), which responses a layer distance of
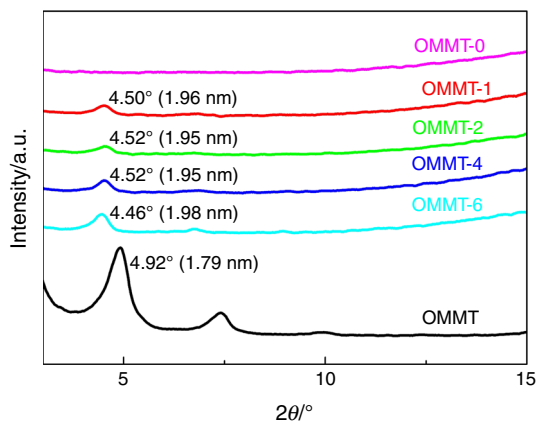
Fig. 2 X-ray diffraction results of OMMT and the OMMT-modified soybean oil-based PU/EP IPNs

1.79 nm. After the interaction with the PU/EP IPNs, layer distance of OMMT increases to an average of 1.96 nm, which indicates the polymer chains to intercalate into the layered construction of OMMT and result in the 10 % distance expansion. This observation is similar to other OMMT-modified PU/EP IPNs [28]. Considering the change of layer distance (about 0.17 nm) and the typical C–C bond length (about 150 pm), it is probable that more than one chains intercalate in the same layer simultaneously, which would promote chain cross-linking.

Morphology

Scanning electron micrographs of the fracture surfaces of the neat soybean oil-based PU/EP IPN and the OMMT-modified PU/EP IPNs are shown in Fig. 3. As demonstrated in Fig. 3a, obviously, the PU/EP IPN contains phase separation, in which epoxy resin is the continuous phase and the spherical PU is the dispersed phase [32]. With the addition of OMMT, the fractured surfaces of PU/EP IPNs become more uneven and rougher, observed in Fig. 3b–e. Moreover, it can be observed that OMMT is homogeneously dispersed in the IPNs, which implies good compatibility and strong interaction between the clay and the polymer matrix [34]. In Fig. 3b, c, no aggregation of OMMT is observed in IPNs. However, when the OMMT mass ratio reaches 4 %, the OMMT particles tend to aggregate. In Fig. 3e, with an OMMT loading of 6 %, the aggregation of OMMT particles becomes very obvious. It is well known that aggregation of clay particles in the polymer matrix would result in adverse influence on the physical properties of polymer nanocomposites [35]. The adverse effects of aggregation will be discussed below (see "Tensile properties" section).
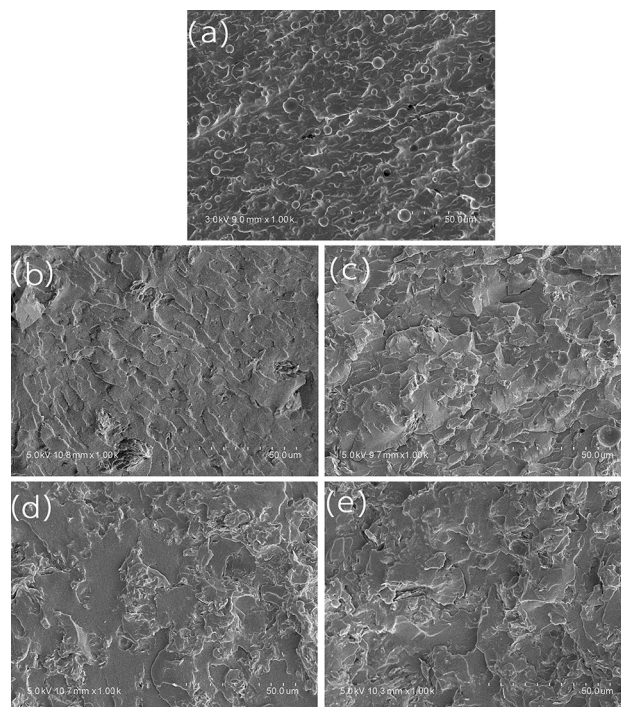

Fig. 3 Scanning electron micrographs of OMMT-0 (**a**), OMMT-1 (**b**), OMMT-2 (**c**), OMMT-4 (**d**), and OMMT-6 (**e**)

Glass transition temperature

The temperature versus loss tangent (tanδ) curves for the OMMT-modified PU/EP IPNs are shown in Fig. 4. T_g is defined as the temperature of maximum tanδ, and the T_gs of the modified PU/EP IPNs are listed in Table 2. Like other PU/EP IPNs [26], only one single glass transition peak is demonstrated in all of the tanδ-temperature curves. It can be seen that the T_gs of the modified IPNs are higher than that of the pure IPN. Though the T_g of OMMT-2 drops back for 1 °C, the T_g of modified IPN tends to increase with the mass ratio of OMMT above 4 %. OMMT-6 has the highest T_g value, which is 12 °C higher than that of the pure PU/EP IPN. As demonstrated in "X-ray diffraction" section, polymer chains intercalated into the clay layers. Being restricted in the distance of 1.96 nm, chain movements and rotations are hindered and chain cross-linking is promoted. Polymer chains are less likely to move, resulting in the increase in the glass transition temperature. This tendency agrees well with the intercalation model of layered clay–polymer nanocomposites [22].

Damping properties

It is well known that some IPNs have been widely used as damping materials, because they have the high tanδ value in
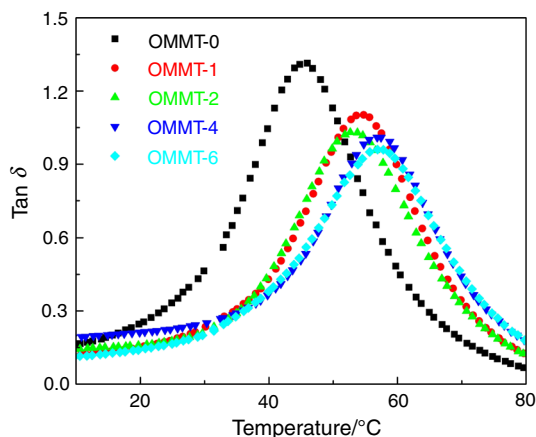
Fig. 4 Temperature dependence of tanδ for the OMMT-modified soybean oil-based PU/EP IPNs

Table 2 T_g and damping properties of the OMMT-modified soybean oil-based PU/EP IPNs

Sample	T_g/°C	$(\tan\delta)_{max}$	ΔT at $\tan\delta > 0.3$/°C	TA/K
OMMT-0	45.2	1.32	41.70 (23.25–64.95)	31.66
OMMT-1	54.4	1.10	36.95 (34.40–71.35)	25.46
OMMT-2	53.4	1.03	35.40 (35.35–70.75)	23.95
OMMT-4	57.1	1.01	38.50 (35.70–74.20)	24.47
OMMT-6	57.4	0.96	37.80 (36.45–74.25)	24.00

a wide temperature range [36]. In the present work, the effect of OMMT on the damping properties of the PU/EP IPNs is estimated by the loss tangent maximum $(\tan\delta)_{max}$, the temperature range (ΔT) for efficient damping ($\tan\delta > 0.3$), and the integral area (TA) under the tanδ curve [32, 37]. All the statistics are listed in Table 2. The $(\tan\delta)_{max}$ and ΔT are 1.32 and 41.7 °C, respectively, which is much higher than many other polymers ($\tan\delta < 0.3$) and indicates the soybean oil-based PU/EP IPN has excellent damping properties. The $(\tan\delta)_{max}$ decreases steadily from 1.32 to 0.96 as the mass ratio of OMMT rises from 0 to 6 %. With the addition of OMMT, both ΔT and TA of PU/EP IPNs decrease slightly. These results may attribute to restriction effect of clay layers on the segmental mobility of polymer chains. Being intercalated in OMMT layers, the restricted polymer chains become rigid and respond slower to external forces. The loss modulus is reduced, leading to a decrease in damping properties. Similar results were also reported in OMMT/linseed oil-based elastomeric bio-nanocomposites [38]. It is worthy to noting that the loss factor and the temperature range for efficient damping ($\tan\delta > 0.3$) of OMMT-modified soybean oil-based PU/EP IPNs are still much higher than those of normal polymers [38].
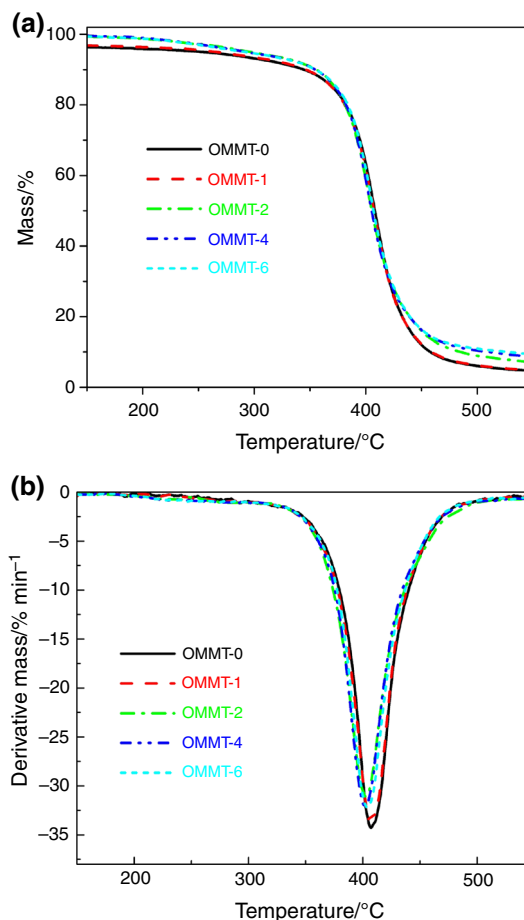

Fig. 5 TG (**a**) and DTG (**b**) curves of OMMT-modified soybean oil-based PU/EP IPNs

Thermal stability

The TG and derivative TG (DTG) curves of the neat soybean oil-based PU/EP IPN and the OMMT-modified IPNs are shown in Fig. 5. Only one stage is observed in the thermal degradation of the soybean oil-based PU/EP IPN and its OMMT nanocomposites, as shown in Fig. 5b. Thermal statistics, including the initial decomposition temperature (IDT, the temperature at 5 % mass loss), the integral procedural temperature (IPDT), the maximum rate of degradation temperatures (T_{max}) and the residue at 550 °C, are listed in Table 3. It can be observed that the incorporation of OMMT increases the IDT of the PU/EP IPNs, especially when the loading of OMMT is higher than 1 %. For IPN with 2 % OMMT, the IDT is 42 °C greater than that of the neat PU/EP IPN. The IPDT represents inherent thermal stability of the polymer matrix and hybrid materials, which relates to the decomposition properties of volatile composition [39]. Obviously, the IPDT of OMMT-modified PU/EP IPNs increases with the increase in clay

Table 3 TG and DTG results of the OMMT-modified soybean oil-based PU/EP IPNs

Sample	IDT/°C	IPDT/°C	T_{max}/°C	Residue at 550 °C/%
OMMT-0	253.9	462.1	407.0	4.6
OMMT-1	266.9	465.8	407.4	4.7
OMMT-2	296.4	481.7	402.6	7.0
OMMT-4	293.8	486.4	402.1	8.6
OMMT-6	291.7	490.0	404.2	9.4

loadings. The IPDT of OMMT-6 is 28 °C higher than that of the pure PU/EP IPNs. It can be seen that the incorporation of OMMT has little effects on the T_{max}. However, the residue at 550 °C of OMMT-modified PU/EP IPNs increases with the increase in OMMT loading. The results above indicate that the addition of OMMT improves the thermal stability of the PU/EP IPNs, which possibly ascribes to the thermal insulation effect of the OMMT [29]. The thermal-insulated OMMT reduces the heating rate of the polymer chains that intercalated in its layers and hence delays the decomposition procedure of the PU/EP IPNs.

Tensile properties

The tensile strength, elongation at peak, and tensile modulus of the OMMT-modified PU/EP IPNs are illustrated in Fig. 6. Evidently, the addition of OMMT significantly improves the tensile strength of IPNs, as shown in Fig. 6a. The tensile strength of IPNs reaches a maximum value at 4 % OMMT loading with an increase of 64 %. As shown in "Morphology" section and Fig. 3, OMMT keeps good homogeneity with low loading. The uniform dispersion of the clay allows the yielding procedure taking place throughout the whole polymer matrix, hence increasing the tensile strength. However, when OMMT aggregates, yielding is no longer homogeneous and the tensile strength of OMMT-6 starts to decrease. Meanwhile, the elongation at peak of PU/EP IPNs significantly decreases with the increment of OMMT mass ratio. However, the tensile modulus grows drastically when 1 mass% OMMT was added. With more OMMT, the increment becomes smooth. The tensile modulus of OMMT-6 is nearly four times of that of the neat PU/EP IPN, while the elongation at peak is only 7 % of it. Compared with the pure PU/EP IPN, the modified PU/EP IPNs are much stiffer but less elastic, especially when OMMT loading is above 4 %. The enhancement in modulus may be owing to the dispersion of OMMT in the polymer matrix, while the intercalation that constricts the polymer chain movements lowers the performance in elongation [40].
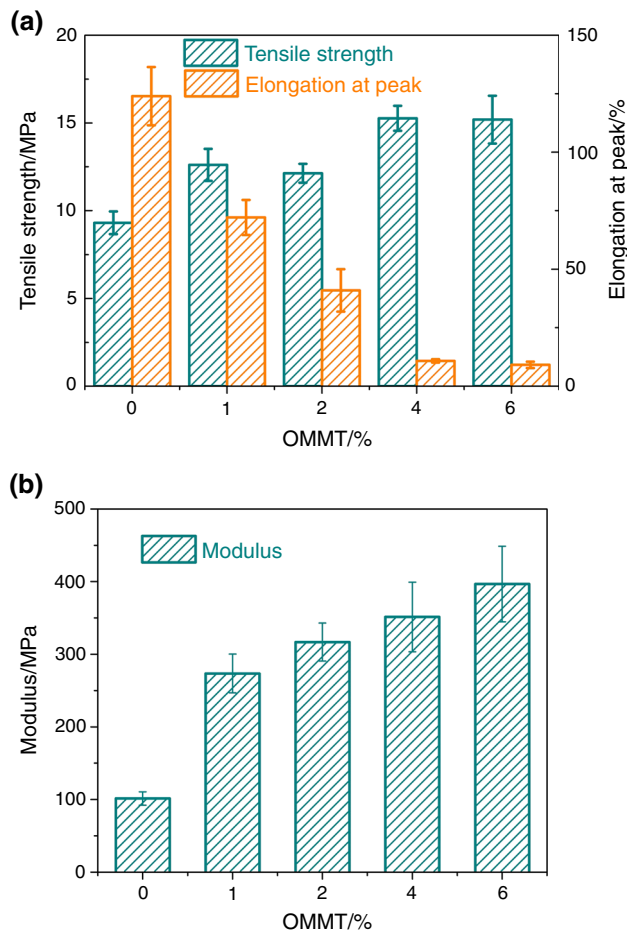
Fig. 6 Tensile properties in tensile strength, elongation at peak (**a**) and tensile modulus (**b**) of the OMMT-modified soybean oil-based PU/EP IPNs

Conclusions

In this work, OMMT was used to modify the soybean oil-based PU/EP IPNs. The effects of OMMT on the structure, morphology, thermal, and mechanical properties of the PU/EP IPNs were investigated. The following conclusions have been drawn:

1. Polymer chains intercalated into the layer gaps of OMMT, resulting in a 10 % expansion of layer distances. The OMMT disperses in the polymer matrix with good compatibility. The structural features contributed to the enhancement in properties of the PU/EP IPNs.

2. The glass transition temperatures of PU/EP IPNs tend to increase with more OMMT loading. However, the addition of OMMT decreases the damping properties of the PU/EP IPNs. The addition of OMMT improves the thermal stability of the PU/EP IPNs.

3. The incorporation of OMMT significantly increases the tensile strength and tensile modulus of the PU/EP IPNs. However, the elongation at peak of the PU/EP IPNs decreases with the increase in OMMT loadings.

References

1. Yin H, Zhang Y, Sun Y, Xu W, Yu D, Xie H, et al. Performance of hot mix epoxy asphalt binder and its concrete. Mater Struct. 2015;48(11):3825–35.
2. Zhang Y, Pan X, Sun Y, Xu W, Pan Y, Xie H, et al. Flame retardancy, thermal, and mechanical properties of mixed flame retardant modified epoxy asphalt binders. Constr Build Mater. 2014;68:62–7.
3. Zhang Y, Sun Y, Xu K, Yuan Z, Zhang J, Chen R, et al. Brucite modified epoxy mortar binders: flame retardancy, thermal and mechanical characterization. Constr Build Mater. 2015;93:1089–96.
4. Thomas S, Thomas R, Sinturel C. Micro and nanostructured epoxy/rubber blends. Weinheim: Wiley; 2014.
5. Wang Y, Wang C, Yin H, Wang L, Xie H, Cheng R. Carboxyl-terminated butadiene–acrylonitrile-toughened epoxy/carboxyl-modified carbon nanotube nanocomposites: thermal and mechanical properties. Express Polym Lett. 2012;6(9):719–28.
6. Zhang J, Wang Y, Wang X, Ding G, Pan Y, Xie H, et al. Effects of amino-functionalized carbon nanotubes on the properties of amine-terminated butadiene–acrylonitrile rubber-toughened epoxy resins. J Appl Polym Sci. 2014;131(13):40472.
7. Sperling LH, Hu R. Interpenetrating polymer networks. In: Utracki LA, Wilkie CA, editors. Polymer blends handbook. Netherlands: Springer; 2014. p. 677–724.
8. Hua FJ, Hu CP. Interpenetrating polymer networks of epoxy resin and urethane acrylate resin: 2. Morphology and mechanical property. Eur Polym J. 2000;36(1):27–33.
9. Dhevi DM, Jaisankar S, Pathak M. Effect of new hyperbranched polyester of varying generations on toughening of epoxy resin through interpenetrating polymer networks using urethane linkages. Eur Polym J. 2013;49(11):3561–72.
10. Chaudhary S, Parthasarathy S, Kumar D, Rajagopal C, Roy PK. Graft-interpenetrating polymer networks of epoxy with polyurethanes derived from poly(ethyleneterephthalate) waste. J Appl Polym Sci. 2014;131(13):40490.
11. Li D, Wang Y, Liu Y, Xie Z, Wang L, Tan H. Preparation and properties of polyurethane-modified epoxy cured in different simulated gravity environments. J Appl Polym Sci. 2015;132(25):42063.
12. Hsieh K, Han J. Graft interpenetrating polymer networks of polyurethane and epoxy. II. Toughening mechanism. J Polym Sci Part B Polym Phys. 1990;28(6):783–94.
13. Pfister DP, Xia Y, Larock RC. Recent advances in vegetable oil-based polyurethanes. ChemSusChem. 2011;4(6):703–17.
14. Liu W, Xu K, Wang C, Qian B, Sun Y, Zhang Y, et al. Carbon nanofibers reinforced soy polyol-based polyurethane nanocomposites. J Therm Anal Calorim. 2016;123(3):2459–68.
15. Wang CS, Chen XY, Xie HF, Cheng RS. Effects of carbon nanotube diameter and functionality on the properties of soy polyol-based polyurethane. Compos Part A Appl Sci. 2011;42(11):1620–6.
16. Wang CS, Wang YT, Liu WJ, Yin HY, Yuan ZR, Wang QJ, et al. Natural fibrous nanoclay reinforced soy polyol-based polyurethane. Mater Lett. 2012;78:85–7.
17. Wang CS, Ding L, Wu QS, Liu F, Wei J, Lu R, et al. Soy polyol-based polyurethane modified by raw and silylated palygorskite. Ind Crop Prod. 2014;57:29–34.
18. Karak N. Vegetable oil-based polymers. Cambridge: Woodhead Publishing Limited; 2012.
19. Chen SB, Wang QH, Wang TM. Damping, thermal, and mechanical properties of carbon nanotubes modified castor oil-based polyurethane/epoxy interpenetrating polymer network composites. Mater Des. 2012;38:47–52.
20. Jia J, Qin Y, Mei Q, Huang Z. Castor oil-Based polyurethane/epoxy intercross-linked polymer network adhesives for metal substrates. J Macromol Sci Part B. 2014;53(10):1621–8.
21. Chen SB, Wang QH, Pei XQ, Wang TM. Dynamic mechanical properties of castor oil-based polyurethane/epoxy graft interpenetrating polymer network composites. J Appl Polym Sci. 2010;118(2):1144–51.
22. Alexandre M, Dubois P. Polymer-layered silicate nanocomposites: preparation, properties and uses of a new class of materials. Mater Sci Eng Rep. 2000;28(1–2):1–63.
23. Giannelis EP, Krishnamoorti R, Manias E. Polymer-silicate nanocomposites: model systems for confined polymers and polymer brushes. Adv Polym Sci. 1999;138:107–47.
24. Usuki A, Kojima Y, Kawasumi M, Okada A, Fukushima Y, Kurauchi T, et al. Synthesis of nylon 6-clay hybrid. J Mater Res. 1993;8(5):1179–84.
25. Bakar M, Lavorgna M, Szymańska J, Dętkowska A. Epoxy/polyurethane/clay ternary nanocomposites–Effect of components mixing sequence on the composites properties. Polym Plast Technol Eng. 2012;51(7):675–81.
26. Chen S, Wang Q, Wang T. Damping, thermal, and mechanical properties of montmorillonite modified castor oil-based polyurethane/epoxy graft IPN composites. Mater Chem Phys. 2011;130(1):680–4.
27. Kostrzewa M, Hausnerova B, Bakar M, Pająk K. Preparation and characterization of an epoxy resin modified by a combination of MDI-based polyurethane and montmorillonite. J Appl Polym Sci. 2011;122(5):3237–47.
28. Jia Q, Zheng M, Shen R, Chen H. Synthesis, characterization and properties of organoclay-modified polyurethane/epoxy interpenetrating polymer network nanocomposites. Polym Int. 2006;55(3):257–64.
29. Jia Q, Shan S, Wang Y, Gu L, Li J. Tribological performance and thermal behavior of epoxy resin nanocomposites containing polyurethane and organoclay. Polym Adv Technol. 2008;19(7):859–64.
30. Bakar M, Kostrzewa M, Hausnerova B, Sar K. Preparation and property evaluation of nanocomposites based on polyurethane-modified epoxy/montmorillonite systems. Adv Polym Technol. 2010;29(4):237–48.
31. Li J. High performance epoxy resin nanocomposites containing both organic montmorillonite and castor oil-polyurethane. Polym Bull. 2006;56(4–5):377–84.
32. Jin H, Zhang YG, Wang CS, Sun YF, Yuan ZR, Pan YQ, et al. Thermal, mechanical, and morphological properties of soybean oil-based polyurethane/epoxy resin interpenetrating polymer networks (IPNs). J Therm Anal Calorim. 2014;117(2):773–81.
33. Dai HH, Yang LT, Lin B, Wang CS, Shi G. Synthesis and characterization of the different soy-based polyols by ring opening of epoxidized soybean oil with methanol, 1,2-ethanediol and 1,2-propanediol. J Am Oil Chem Soc. 2009;86(3):261–7.
34. Sun YF, Xu K, Zhang YG, Zhang J, Chen R, Yuan ZR, et al. Organic montmorillonite reinforced epoxy mortar binders. Constr Build Mater. 2016;107:378–84.

35. Leszczynska A, Njuguna J, Pielichowski K, Banerjee JR. Polymer/montmorillonite nanocomposites with improved thermal properties. Part I. Factors influencing thermal stability and mechanisms of thermal stability improvement. Thermochim Acta. 2007;453(2):75–96.

36. Trakulsujaritchok T, Hourston D. Damping characteristics and mechanical properties of silica filled PUR/PEMA simultaneous interpenetrating polymer networks. Eur Polym J. 2006;42(11): 2968–76.

37. Yin HY, Jin H, Wang CS, Sun YF, Yuan ZR, Xie HF, et al. Thermal, damping, and mechanical properties of thermosetting epoxy-modified asphalts. J Therm Anal Calorim. 2014;115(2): 1073–80.

38. Das R, Kumar R, Banerjee SL, Kundu P. Engineered elastomeric bio-nanocomposites from linseed oil/organoclay tailored for vibration damping. RSC Adv. 2014;4(103):59265–74.

39. Gao M, Yang SS. A novel intumescent flame-retardant epoxy resins system. J Appl Polym Sci. 2010;115(4):2346–51.

40. Yasmin A, Abot JL, Daniel IM. Processing of clay/epoxy nanocomposites by shear mixing. Scr Mater. 2003;49(1):81–6.